A COMPARISON OF RECURSIVE LEAST SQUARES AND KALMAN FILTERING EXCISORS FOR SWEPT TONE INTERFERENCE

by

Brian Kozminchuk

DEFENCE RESEARCH ESTABLISHMENT OTTAWA
TECHNICAL NOTE 92-14

Canada

October 1992
Ottawa

National Défense
Defence nationale

A COMPARISON OF RECURSIVE LEAST SQUARES AND KALMAN FILTERING EXCISORS FOR SWEPT TONE INTERFERENCE

by

Brian Kozminchuk
Communications Electronic Warfare Section
Electronic Warfare Division

DEFENCE RESEARCH ESTABLISHMENT OTTAWA
TECHNICAL NOTE 92-14

PCN
041LK11

October 1992
Ottawa

ABSTRACT

This technical note presents a Kalman filtering approach that is used for filtering narrowband interferers out of direct sequence spread spectrum signals. The approach is based on the digital phase-locked loop Kalman filter and is close to optimum in so far as demodulating an FM-type of interferer. Because the interference is assumed to be much stronger than either the signal or noise, the Kalman filter locks onto the interference and produces estimates of its phase and envelope. The algorithm is compared, through computer simulation, with the recursive least squares lattice algorithm for the case of a swept tone interferer. Examples of the phase- and envelope-tracking capabilities of the algorithm are presented, followed by bit error rate curves for the case of an interferer of bandwidth equal to 20% of the chip rate of the spread spectrum signal. The results show that with proper selection of the Kalman filter parameters, the Kalman filter excisor can outperform the recursive least squares algorithm by 2 dB. It is suggested that performance could perhaps be improved further by using a higher order Kalman filter to remove the residual phase-tracking error produced by the second order Kalman filter.

RÉSUMÉ

Ce rapport contient une description d'un filtrage de Kalman utilisé pour enlever des interférences à bande passante étroite d'un signal à spectre étalé par une séquence directe. La méthode repose sur un filtre de Kalman à verrouillage numérique de phase et est presque optimale pour la démodulation d'interférences de type FM. Le filtre de Kalman se verrouille sur l'interférence et produit une estimation de sa phase et de son envelope parce que l'on suppose que l'interférence et le bruit sont beaucoup plus forts que le signal. Une simulation par ordinateur est utilisée pour comparer ce filtre à la méthode des treillis des moindres carrés récursifs pour une interférence à balayage de fréquence. On présente des exemples de poursuites de phase et d'enveloppe par l'algorithme ainsi que des courbes de taux d'erreur des bits pour une interférence dont la bande passante est de 20% du débit numérique du signal à spectre étalé. Il est démontré qu'une sélection judicieuse des paramètres du filtre de Kalman permet une excision meilleure que celle produite par l'algorithme récursif des moindres carrés par 2 dB. Il est suggéré qu'une amélioration supplémentaire pourrait être obtenue par l'utilisation d'un filtre de Kalman d'ordre supérieur qui enlèverait ce qui reste de l'erreur de phase d'un filtre de Kalman de second ordre.

EXECUTIVE SUMMARY

This technical note presents a Kalman filtering approach that is used for filtering narrowband interferers out of direct sequence spread spectrum signals. These signals are used extensively in military communication systems. The technique described herein applies equally to both Electronic Support Measures (ESM) systems and direct sequence spread spectrum communication sytems. In the former application, the ESM system may be attempting to intercept the spread spectrum signal, but the narrowband interference may be hampering this effort. In the latter application, the spread spectrum communication system may require additional assistance to suppress the interference. Since the open literature has been devoted to this latter case, the material presented here focuses on this application.

One of the attributes of direct sequence spread spectrum communication systems is their ability to combat interference or intentional jamming by virtue of the system's processing gain inherent in the spreading and despreading process. The interference can be attenuated by a factor up to this processing gain. In some cases the gain is insufficient to effectively suppress the interferer, leading to a significant degradation in communications manifested by a sudden increase in bit error rate. If the ratio of interference bandwidth to spread spectrum bandwidth is small, the interference can be filtered out to enhance system performance. However, this is at the expense of introducing some distortion onto the signal. This process of filtering is sometimes referred to as interference excision.

The Kalman filtering approach is based on the digital phase-locked loop Kalman filter and is close to optimum in so far as demodulating an FM-type of interferer. Because the interference is assumed to be much stronger than either the signal or noise, the Kalman filter locks onto the interference and produces an estimate of the phase and envelope of the interference.

The algorithm is compared, through computer simulation, with the recursive least squares lattice algorithm for the case of a swept tone interferer. Examples of the phase- and envelope-tracking capabilties of the algorithm are presented, followed by bit error rate curves for the case of an interferer of bandwidth equal to 20% of the chip rate of the spread spectrum signal. The results show that with proper selection of the Kalman filter parameters, the Kalman filter excisor can outperform the recursive least squares algorithm by 2 dB and that performance could perhaps be improved further by using a higher order Kalman filter to remove the residual phase-tracking error produced by the second order Kalman filter used in this study.

TABLE OF CONTENTS

LIST OF FIGURES

1.0 INTRODUCTION

Direct sequence spread spectrum communication systems have an inherent processing gain which can reduce the effects of jammers or unintentional interference. When these intruding signals have a power advantage over the spread spectrum system, a severe degradation in communications results. However, communications can be enhanced somewhat by filtering the interference, particularly if its bandwidth is significantly less than the bandwidth of the spread spectrum signal.

A host of digital filtering algorithms based on time-modelling concepts have been developed over the years to address this problem [1, 2, 3]. The received signal, noise and interference are applied, for example, to a filter matched to a chip and the output is sampled at the chip rate. If one assumes that the resulting sampled data can be modelled as an autoregressive (AR) process, then the AR coefficients or their related lattice reflection coefficients can be determined from, say, the maximum entropy algorithm [4], stochastic gradient algorithms [5], and block and recursive least squares algorithms [6, 7]. Estimates of these coefficients by the above algorithms lead directly to transversal or lattice filter structures, both of which act as whitening filters for the assumed AR process. This approach to suppressing interference (or excision as it is sometimes referred to) is possible because of the non-coherency of the signal and noise samples, and the more coherent interference samples resulting from the latter's narrowband nature.

A different time-modelling approach to interference excision was presented in [8]. There, a function related to the interference is assumed to have been generated by a second order state-space system to which the extended Kalman filter equations are applied. This results in what has been termed the digital phase-locked loop (DPLL) [9, 10]. This approach to interference suppression is close to optimum for the suppression of constant envelope or FM-types of interferers and, therefore, can potentially provide better performance than the recursive least squares (RLS) algorithm which was analyzed for the swept tone in [11]. The objective of this technical note is to present a performance comparison between the DPLL and RLS algorithms for the swept tone interferer.

The outline of this technical note is as follows. Section 2.0 describes the spread spectrum communication model and interference estimator based on the Kalman filter. Section 3.0 summarizes the interference estimator. Section 4.0 presents simulation results for the case of a swept tone interferer corrupting the spread spectrum signal. The Kalman filtering approach is compared to the lattice RLS algorithm previously discussed [11]. Finally, Section 5.0 concludes the technical note, suggesting areas for further research.

2.0 COMMUNICATIONS MODEL

The basic elements of the BPSK PN spread spectrum receiving system are shown in Fig. 1. The received waveform $r(t)$, consisting of a spread spectrum signal, additive

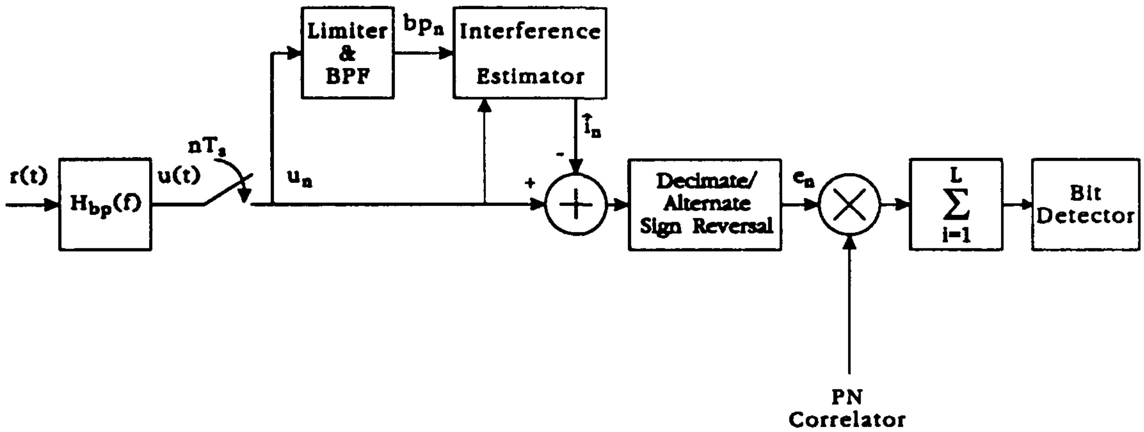

Figure 1: Spread spectrum communications model.

white Gaussian noise, and narrowband interference is applied to a bandpass filter with the transfer function $H_{bp}(f)$, whose output is defined as

$$u(t) = s(t) + n(t) + i(t). \tag{1}$$

The bandpass filter $H_{bp}(f)$, for the application considered here, is assumed to be a filter matched to a chip and centered at the carrier angular frequency ω_0 of the spread spectrum signal. The spread spectrum signal is defined as

$$s(t) = a(t)\cos(\omega_0 t) \tag{2}$$

where

$$a(t) = \sum_k D_k b_k(t - kT_b). \tag{3}$$

In Eq. (3), D_k is a sequence of data bits of amplitude (± 1) and duration T_b seconds, and $b_k(t - kT_b)$ is the PN sequence pattern for the k^{th} bit, i.e.,

$$b_k(t) = \sum_{j=1}^{L} c_{kj} q(t - jT_c) \tag{4}$$

with L being the number of pseudo random chips per bit, or the processing gain, c_{kj} is the code sequence for the bit, and $q(t)$ represents the basic chip pulse of energy E_c.

The noise $n(t)$ is Gaussian and has a power spectral density

$$S_n(f) = \frac{N_0}{2}|H_{bp}(f)|^2, \tag{5}$$

where $N_0/2$ is the power spectral density of the assumed white Gaussian noise from the channel. The band of interference is defined as

$$i(t) = I(t)\cos(\omega_0 t + \theta(t)) \tag{6}$$

where $I(t)$ is the interference amplitude and $\theta(t)$ is the phase modulation. It has been assumed that the effect of the bandpass filter $H_{bp}(f)$ is negligible on the interference $i(t)$. This would not be true in reality, since the bandpass filter will induce some amplitude modulation on the constant envelope interference. The rate of change of the envelope would therefore depend on the rate of change of the instantaneous frequency, and the amplitude deviation would depend on the frequency offset from ω_0 and the interference bandwidth. The fact that this report considers the amplitude to be of constant envelope at the output of the bandpass filter corresponds to the best case situation.

Referring to Fig. 1, the output $u(t)$ of the bandpass filter $H_{bp}(f)$ is bandpass sampled and applied to a limiter/bandpass filter and interference estimator.

Consider the bandpass sampler first. The analog signal $u(t)$ from Eq. (1) is sampled at $f_s = 2R_c$ ($mf_s = \omega_0/2\pi + R_c/2$ for some integer m) where R_c is the chip rate of the spread spectrum signal. The resultant sampled signal is, therefore,

$$u_n = s_n + n_n + i_n, \tag{7}$$

where s_n consists of the sequence $\{\ldots, 0, (-1)^n a_n, 0, (-1)^{n+2} a_{n+2}, \ldots\}$ where the a_n are of energy E_c and coded according to $c_{kj}D_k$ for the j^{th} chip in the k^{th} transmitted bit, n_n [1] are uncorrelated Gaussian noise samples of variance $\sigma_{nse}^2 = E_c(N_0/2)$, and i_n is the sampled version of Eq. (6). The samples u_n are applied to the interference estimator and interference canceller.

The interference estimator produces an estimate $\hat{i}_n$ of the interference which is removed from the sampled input u_n. The output of the summer is decimated and sign-reversed, resulting in a baseband error signal e_n. This error signal is correlated with the

[1]Coherent bandpass sampling has been assumed, so that the in-phase component is $(n_{1,n}/\sqrt{2})\cos(n\pi/2)$ and the quadrature component is $(n_{2,n}/\sqrt{2})\sin(n\pi/2)$

PN sequence. The output of the correlator is integrated and bit-detected.

3.0 INTERFERENCE ESTIMATOR

Consider now the branch containing the limiter. Here, u_n is applied to a limiter/bandpass filter. The input to the limiter referenced to the interference is redefined as

$$u_n = \sqrt{[I_n + n'_{1,n} + a'_{1,n}]^2 + [n'_{2,n} + a'_{2,n}]^2} \cos[\omega_0 n + \theta_n + \phi_{u,n}] \tag{8}$$

where

$$\phi_{u,n} = \arctan\left(\frac{n'_{2,n}/\sqrt{2} + a'_{2,n}}{I_n + n'_{1,n}/\sqrt{2} + a'_{1,n}}\right) \tag{9}$$

is a noise-like phase fluctuation on the interferer's phase θ_n, and is due to the noise and spread spectrum signal. The terms $n'_{1,n}$, $n'_{2,n}$, $a'_{1,n}$, and $a'_{2,n}$ are in-phase and quadrature components of the noise and spread spectrum signal with respect to the interference phase θ_n.

The output of the limiter/bandpass filter is [12]

$$bp_n = \frac{4A'}{\pi} \cos[\omega_0 n + \theta_n + \phi_{u,n}], \tag{10}$$

where A' is the limiter's output level. This signal is redefined as (letting $A' = \sqrt{2}\pi/4$ for convenience)

$$bp_n = \sqrt{2} \cos[\omega_0 n + \theta_n + \phi_{u,n}]. \tag{11}$$

It should be noted that for large interference-to-noise ratios in which the interference is of constant envelope, $\phi_{u,n}$ in Eq. (11) is approximately Gaussian [12]. The sampled signal in Eq. (11) is what is processed by the Kalman filter, which estimates the phase θ_n of the interference. The phase estimate is denoted as $\hat{\theta}_{n|n-1}$

The interference estimator shown in Fig. 1 is detailed in Fig. 2. The Kalman algorithm [8] produces a signal

$$\hat{y}_n = \sqrt{2} \cos(\omega_0 n + \hat{\theta}_{n|n-1}) \tag{12}$$

which can be used as a basis for estimating a sampled version of the envelope of $i(t)$ (i.e., I_n in Eq. (6)). The output of the first multiplier is a baseband term and is, using Eq. (7), excluding the $\sqrt{2}$ factor,

$$\hat{I'}_n = I_n \cos(\theta_n - \hat{\theta}_{n|n-1})$$

$$
\begin{aligned}
&+ \quad n_n \cos(\omega_0 n + \hat{\theta}_{n|n-1}) + a_n \cos(\hat{\theta}_{n|n-1}) \\
&+ \quad a_n \cos(2\omega_0 n + \hat{\theta}_{n|n-1})
\end{aligned} \tag{13}
$$

Equation (13) consists of four terms: the first term is related to the desired envelope of

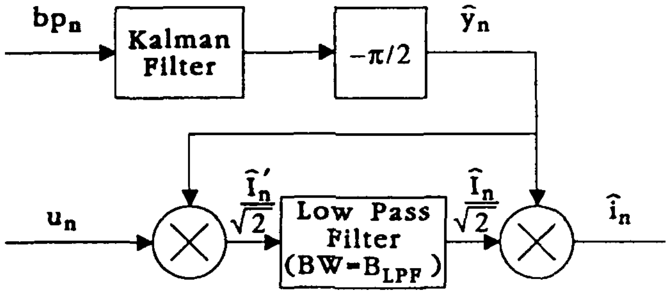

Figure 2: Block diagram of the interference estimator.

the interference; the second is approximately Gaussian baseband noise [13]; and the third and fourth terms are noise-like terms emanating from the spread spectrum signal. The fourth term, because of the sampling rate conditions discussed in [9], is essentially filtered out by the low pass filter of bandwidth $B_{LPF} < 0.50$ Hz and, therefore, will be ignored in the baseband simulations to be discussed in the next section. The term $\hat{I}'_n/\sqrt{2}$ is filtered, resulting in the estimate of the interference envelope, $\hat{I}_n/\sqrt{2}$. Combining this with $\hat{y}_n$ in Eq. (12) and shown in Fig. 2 yields, the estimate of the interference

$$
\hat{i}_n = \hat{I}_n \cos(\omega_0 n + \hat{\theta}_{n|n-1}), \tag{14}
$$

which is subtracted from u_n as illustrated in Fig. 1.

4.0 SWEPT TONE PERFORMANCE

The objective of this section is to compare the performance of the Kalman filter excisor to the RLS algorithm [11] for the case of a swept tone interferer. For this comparison, the Kalman filter is not adaptive; an adaptive architecture will be discussed in another technical note. It is intended here to illustrate the potential performance of the Kalman filtering approach. The modified Kalman algorithm [8] is the one that will be used.

From [8] the performance of the Kalman filter is governed by three parameters. These are the frequency deviation constant d, the variance of the observation noise $\sigma_v^2 = N_{obs}/2$ assumed in the model where $N_{obs}/2$ is the two-sided power spectral density of the observation noise, and the 3 dB bandwidth, α_f, of a low pass filter for filtering white

Gaussian noise to produce the interferer's modulating signal. It is important to note that α_f, which is related to $\gamma = f_s/\alpha_f$, the ratio of the sampling rate to this bandwidth, establishes a family of performance curves such as those in [9]. Thus, for a given α_f and f_s, the approach to be taken will be to determine that value of d which minimizes the mean-squared value of the residual interference in front of the PN correlator in Fig. 1. It is assumed here that for small enough B_{LPF} in Fig. 2, the main source for residual interference will be the phase-noise. Therefore, using the minimum mean-squared value of the residual interference as the criterion for optimality, the value of d determined would provide as close to the optimum performance achievable. Finally, the variance parameter for the observation noise, σ_v^2, will be set according to the noise level in the experiment. This noise level, as shown below, is a function of the power spectral densities of the channel noise and spread spectrum signal.

For this experiment, the interference is modelled as a frequency modulated waveform of the type

$$\begin{aligned} i(t) &= I\cos(\omega_0 t + \theta(t)) \\ &= I\cos(\omega_0 t + 2\pi\delta f t + d\int_0^t m(\tau)d\tau + \varphi) \end{aligned} \tag{15}$$

where δf is an offset frequency from the spread spectrum signal carrier, $m(\tau)$ is the modulating signal of the interferer, d is the frequency deviation constant of the modulator in radians/second/volt [14], and φ is an initial random phase. The swept tone with sweep rates of ± 0.001 Hz/sec. was modelled using Eq. (15). A section of the instantaneous frequency [2] $\dot{\theta}(t)/2\pi$ from Eq. (15) is shown in Fig. 3, sweeping between 0.1 and 0.3 Hz, with $\delta f = 0.2$ Hz and $d = 0.628$ radians/second/volt. With this sweep rate and the values of B_{LPF} used in Fig. 2, it is assumed that the envelope variation at the output of the bandpass filter is slow enough to render the constant envelope assumption valid. The peak frequency deviation Δf for this case was 0.1 Hz and the interference-to-noise ratio was set at 20 dB.

Concerning the other parameters of the experiment, the processing gain was set at $L = 20$ and the energy/chip was $E_c = 1$ unit. For the Kalman filtering approach, the excisor used is the one in Fig. 1, with the interference estimator as shown in Fig. 2. In the latter figure, the low pass filter is of the 4^{th} order Butterworth type of bandwidth B_{LPF}, and is a variable in the simulations. For the RLS excisor, one can refer to [11].

[2]In the simulations that follow, the carrier frequency f_0 has been assumed to be zero, i.e., baseband models have been used.

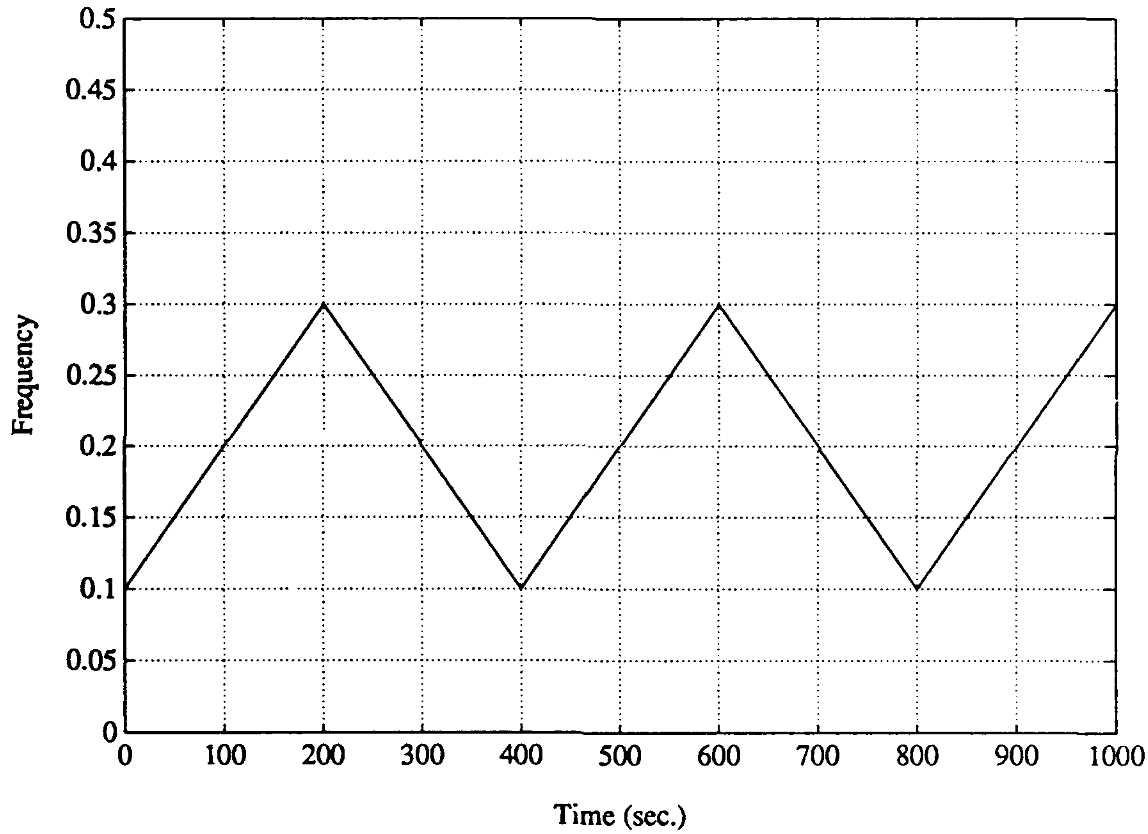

Figure 3: Modulating signal $m(\tau)$ in Eq. (15).

The experiment consists of two parts. The first part is concerned with determining from simulation the optimum value of d for a particular σ_v^2. The second part is concerned with obtaining the bit error rate curve for the swept tone interferer using this optimum value of d, while modifying σ_v^2 in relation to the particular E_b/N_0.

4.1 Optimum d Determination

For fixed α_f and f_s, it suffices to determine the value of the power spectral density of the observation noise $\sigma_v^2 = N_{obs}/2$ to be used in the Kalman filter before varying d to obtain the optimum value. This is accomplished as follows.

The interference-to-noise ratio INR in the equivalent noise bandwidth of the filter of 3 dB bandwidth α_f in the Kalman filter interference model in [9] is

$$INR = \frac{2}{\pi \alpha_f N_{obs}}. \tag{16}$$

From Eq. (9), the phase-noise at the output of the limiter and bandpass filter was defined as

$$\phi_{u,n} = \arctan\left(\frac{n'_{2,n}/\sqrt{2} + a'_{2,n}}{I + n'_{1,n}/\sqrt{2} + a'_{1,n}}\right) \tag{17}$$

where I has replaced I_n, since a constant envelope interferer is being considered. In Eq. (17), using the definition for the signal and noise from Eq. (7), the noise and spread spectrum signal referenced to the phase of the interference become

$$n'_{1,n} = n_{1,n}\cos(\theta_n) + n_{2,n}\sin(\theta_n) \tag{18}$$

$$n'_{2,n} = n_{2,n}\cos(\theta_n) - n_{1,n}\sin(\theta_n) \tag{19}$$

$$a'_{1,n} = a_n\cos(\theta_n) \tag{20}$$

$$a'_{2,n} = -a_n\sin(\theta_n). \tag{21}$$

For $I \gg (s_n + n_n)$, Eq. (17) simplifies to

$$\phi_{u,n} \approx \left(\frac{n'_{2,n}/\sqrt{2} + a'_{2,n}}{I}\right). \tag{22}$$

The approximate mean-squared value of the phase-noise is, therefore,

$$E\{\phi_{u,n}^2\} \;\approx\; (N_0/2 + 0.5)/I^2$$

$$\approx \ \sigma_v^2 = N_{obs}/2 \tag{23}$$

where the 0.5 in Eq. (23) refers to the mean-squared value of the signal term in Eq. (22). It can be seen from Eq. (23) that the variance of the observation noise, σ_v^2, in the Kalman filter model is a function of the channel noise power spectral density N_0, the power in the spread spectrum signal, and the power in the interference.

The kind of performance that can be achieved with the Kalman filter using particular values for σ_v^2 and α_f while varying d is considered next. For this example N_0 (and therefore σ_v^2 from Eq. (23)) was determined from $E_b/N_0 = 12$ dB, α_f was set to a value of 0.0003125 Hz, which corresponds to the value used in [9], d ranged from 0.1 to 2.0 rad./sec./volt, and the bandwidth of the low pass filter designated as B_{LPF} in Fig. 2 was either 0.10 or 0.025 Hz.

Figure 4 shows estimates of the degree of interference suppression at the output of the Kalman filter excisor, where suppression is defined as

$$\mathcal{S} = 10 \log(\overline{\Delta i_n^2}/P_i) \tag{24}$$

where $\Delta i_n = i_n - \hat{i}_n$ is the residual interference, and P_i is the power in the interference. The number of samples used in determining the estimate of $\mathcal{S}$ in Eq. (24) was 20,000. Observe that the "optimum" value for d is ≈ 0.20 rad./sec./volt.

From Eq. (24) and the results in Fig. 4, the efficiency of the excisor, η, defined in Eq. (61a) in [11] can be determined from

$$\eta = \frac{1}{\sigma_{nse}^2/\rho_0 + \mathcal{S}} \tag{25}$$

where, for the case considered here, $\sigma_{nse}^2 = N_0/2$ and $\rho_0 = P_i$. This can be seen by noting that, for the linear prediction approach for which this equation was developed [11], the overall noise term σ^2 in Eq. (61a) in [11] can also be expressed as

$$\sigma^2 = \sigma_{nse}^2 + E\{\Delta i_n^2\}. \tag{26}$$

It should be noted, however, that Eq. (25) for the Kalman filter excisor is only approximate, with the accuracy improving as the bandwidth of the lowpass filter in Fig. 2 becomes significantly less than the sampling rate f_s. Under these latter conditions, the cross-correlation between the residual interference and the signal and noise components (which is zero for the linear prediction case) at the output of the excisor becomes small.

As an example of the amount of efficiency that can be achieved using Eq. (26), for $E_b/N_0 = 12$ dB, $I/S = 20$ dB and $\mathcal{S} = -22$ dB at $d = 0.20$ rad./sec./volt in Fig. 4, $\eta = 19$ dB.

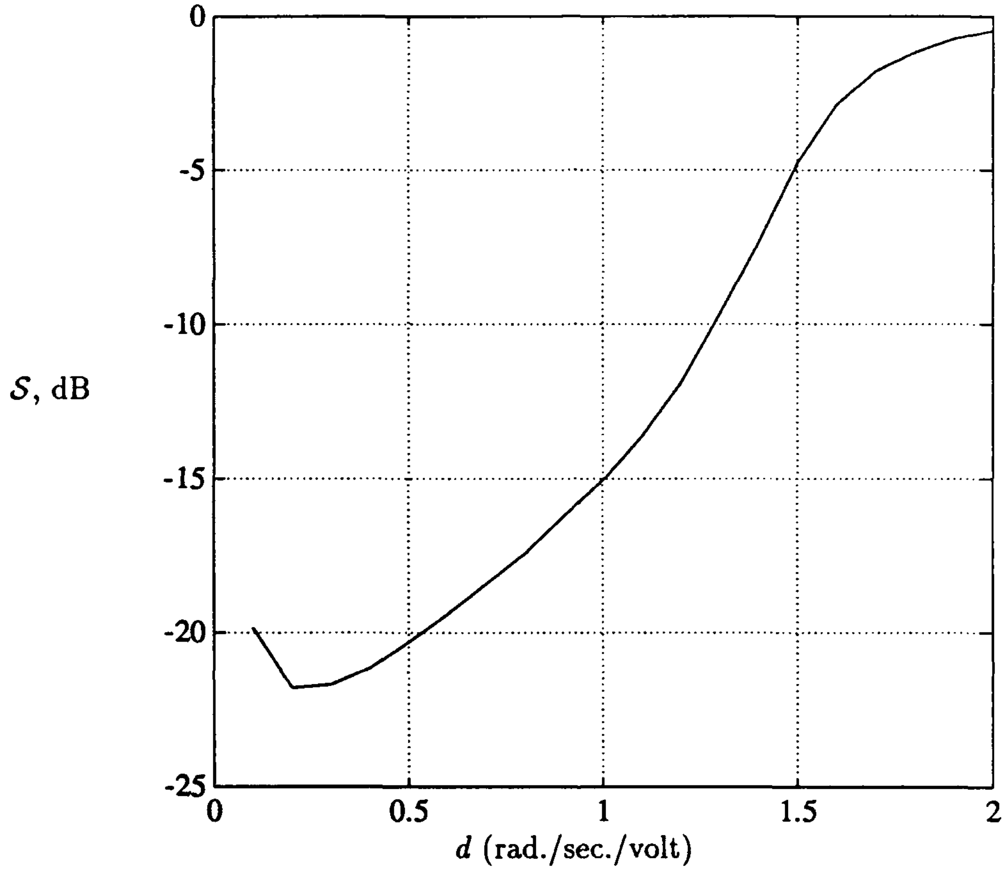

Figure 4: Suppression level $\mathcal{S}$ from Eq. (24) for several values of d, and $B_{LPF} = 0.1$ Hz.

An example of the phase-tracking capability of the Kalman filter for the swept tone interferer is illustrated in Fig. 5, using the optimum value of $d = 0.20$ rad./sec./volt from Fig. 4. There is a slight offset of the phase estimate $\hat{\theta}_{n|n-1}$ from the exact phase θ_n. This offset is 2π radians and is due to initial cycle slippage of the Kalman filter. Furthermore, because of the nonlinearly varying form of the phase (it has a "sinusoidal" feature to it superimposed on a ramp of slope $2\pi(0.2)T_s$ radians/sec. — refer to Eq. (15) and the modulating signal in Fig. 3), the estimate moves closer and further away from the exact phase. This phenomenon is better illustrated in Fig. 6 which shows the phase error $\theta_n - \hat{\theta}_{n|n-1}$, with the initial 2π offset removed, and is due to the inability of the modified

Kalman filter to track nonlinear phase functions without some residual phase error.

The envelope-tracking capability of the interference estimator of Fig. 2 is illustrated in Fig. 7 for two cases: $B_{LPF} = 0.10$ and 0.025 Hz. Observe that by using a smaller value of B_{LPF}, the envelope noise has decreased, which is to be expected, but at the expense of a longer time constant.

Finally, the power spectra for the interference and its estimate are illustrated in Fig. 8. The accuracy of the estimate is excellent in the region of the spectrum where most of the interference power is located; beyond this region one can see the inaccuracies imposed by the noise due to both envelope and phase-noise.

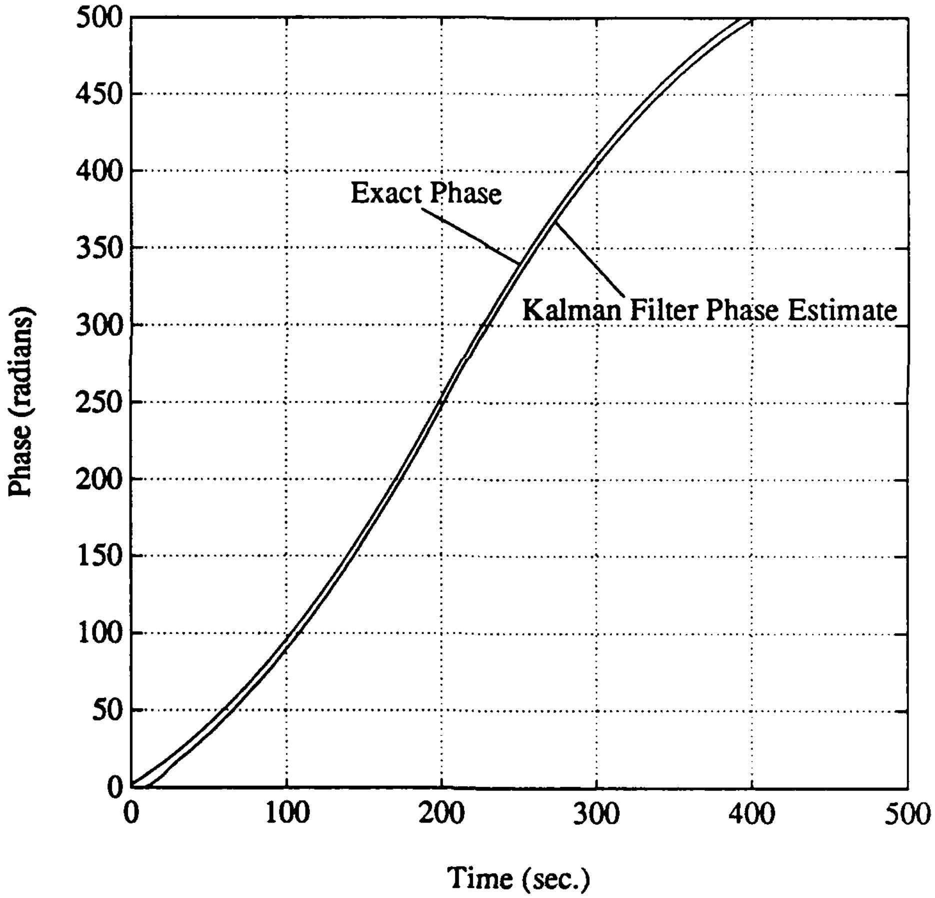

Figure 5: An example of the phase-tracking ability of the Kalman filter for $d = 0.20$ rad./sec./volt, and $B_{LPF} = 0.10$ Hz.

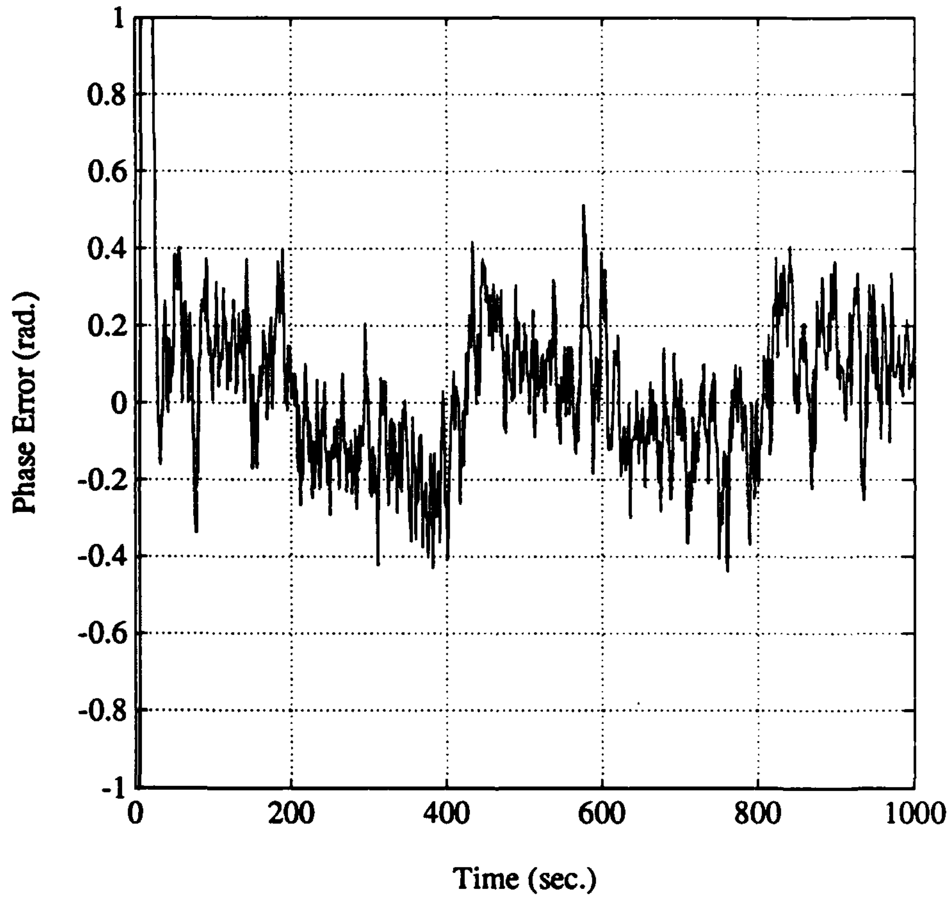

Figure 6: An example of the phase error θ_n - $\hat{\theta}_{n|n-1}$ for d = 0.20 rad./sec./volt, and $B_{LPF} = 0.10$ Hz.

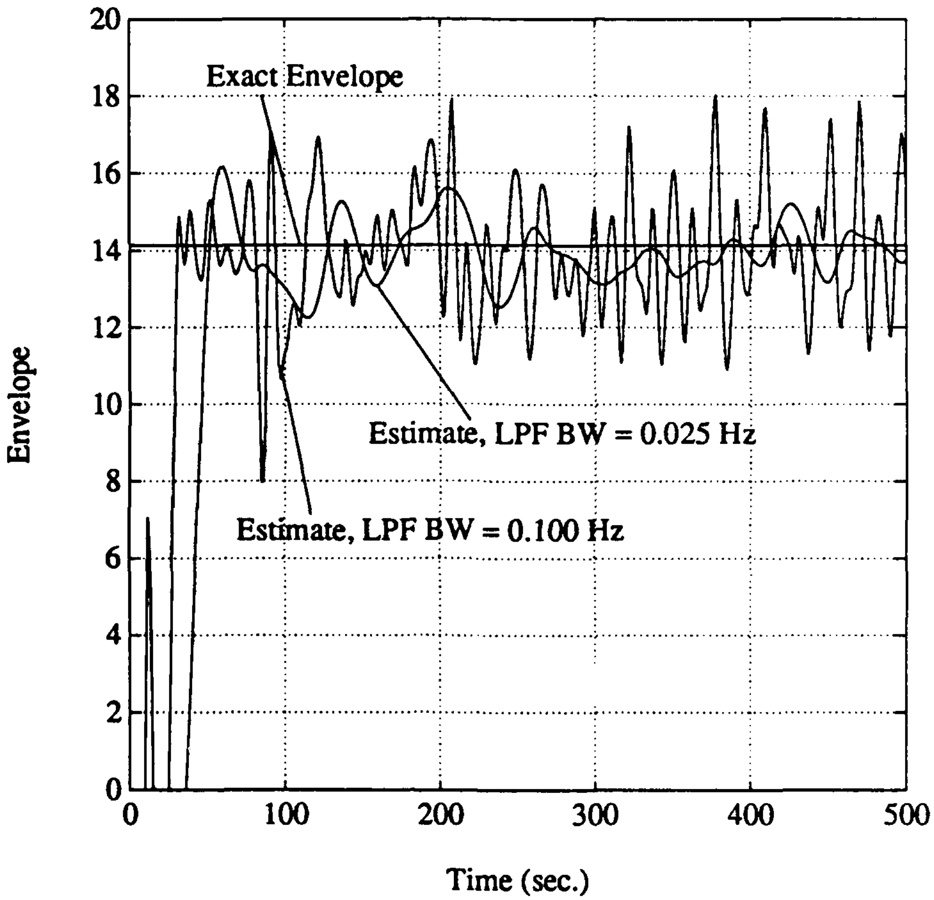

Figure 7: An example of the envelope estimator for $d = 0.20$ rad./sec./volt, and $B_{LPF} =$ 0.10 and 0.025 Hz.

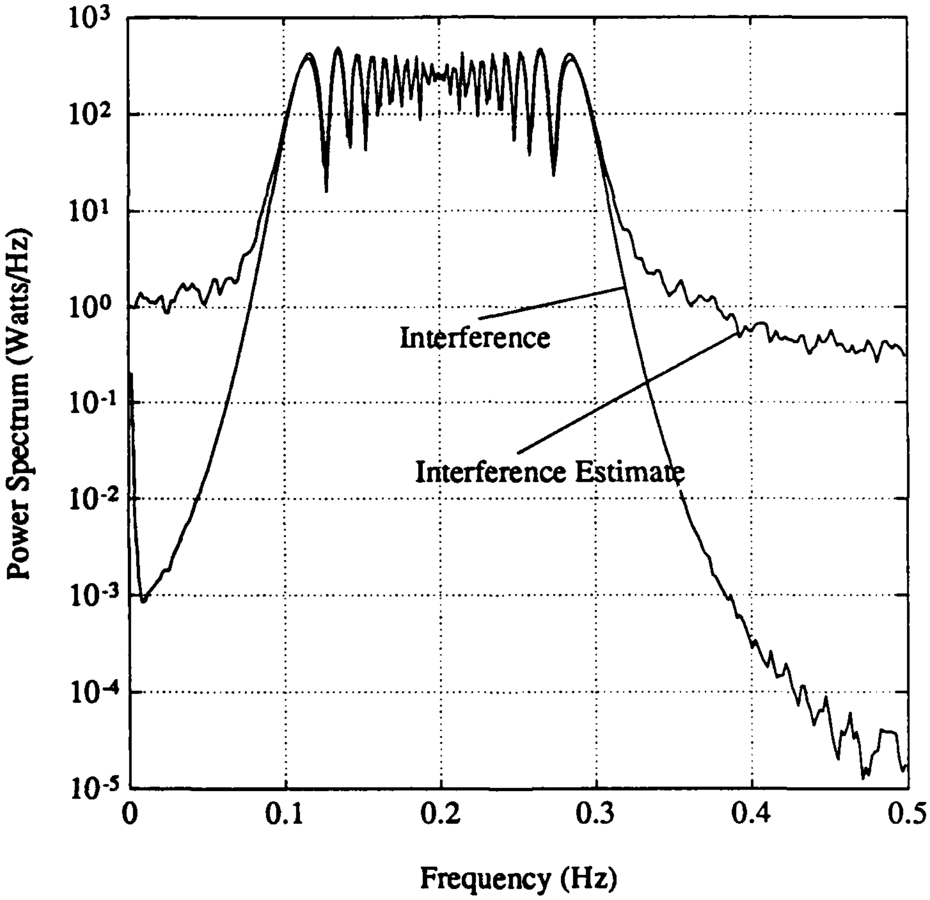

Figure 8: Power spectrum of the interference and its estimate for $d = 0.2$ rad./sec./volt, and $B_{LPF} = 0.1$ Hz.

4.2 Bit Error Rate Performance

In this section the bit error rate performance of the Kalman filter is compared with the RLS algorithm discussed in [11]. For the simulation, a total of 50,000 bits were transmitted (1,000,000 chips), with E_b/N_0 ranging from 0 to 12 dB. The Kalman filter parameters were set up as follows: $\alpha_f = 0.0003125$ Hz, $d = 0.20$ rad./sec./volt (i.e., the optimum value from Fig. 4), and a range of values for σ_v^2, which were calculated from Eq. (23) for the different values of E_b/N_0. Finally, the lowpass filter B_{LPF} in Fig. 2 used to estimate the envelope I of the interference, was 0.10, 0.05 and 0.025 Hz. The parameters of the RLS algorithm were the same as those used in [11].

The results are illustrated in Fig. 9. They indicate that, for the values of B_{LPF} used, the Kalman filter performs better than the RLS algorithm with its matched filter. In fact, the improvement in performance gets progressively better as B_{LPF} decreases. However, there is little noticeable difference between $B_{LPF} = 0.05$ Hz and $B_{LPF} = 0.025$ Hz, suggesting that the residual phase error and phase-noise, both from the Kalman filter, as opposed to the additive noise, and, to some degree, signal distortion, are the main contributors to the lower bound in performance. Considering the nonlinear phase function which the Kalman filter is attempting track, it would be interesting to see if a higher order Kalman filter could provide even better bit error rate performance.

5.0 CONCLUSIONS

This technical note presented some of the performance capabilities of the Kalman filter excisor as applied to a swept tone interferer with interference-to-signal ratio equal to 20 dB. The Kalman filter technique is close to optimum for this type of interference as compared to the RLS excisor, although the latter technique can produce good results if the whitening filter is followed by its matched filter.

It was demonstrated that the Kalman filter can outperform the RLS algorithm, at least for the parameters considered and the assumputions made. It was argued that the limitation in performance in the case of the Kalman filter was due to the phase-noise and the residual phase error caused by the nonlinear phase function being tracked. To remove the residual phase error, one would have to resort to a third order Kalman filter, thus approaching the optimum excisor for this type of interference.

Finally, there would be some difference in performance due to the bandpass filter at the receiver input. To establish how much would be related to the interference parameters; one would have to simulate the effect of this matched filter to obtain precise results.

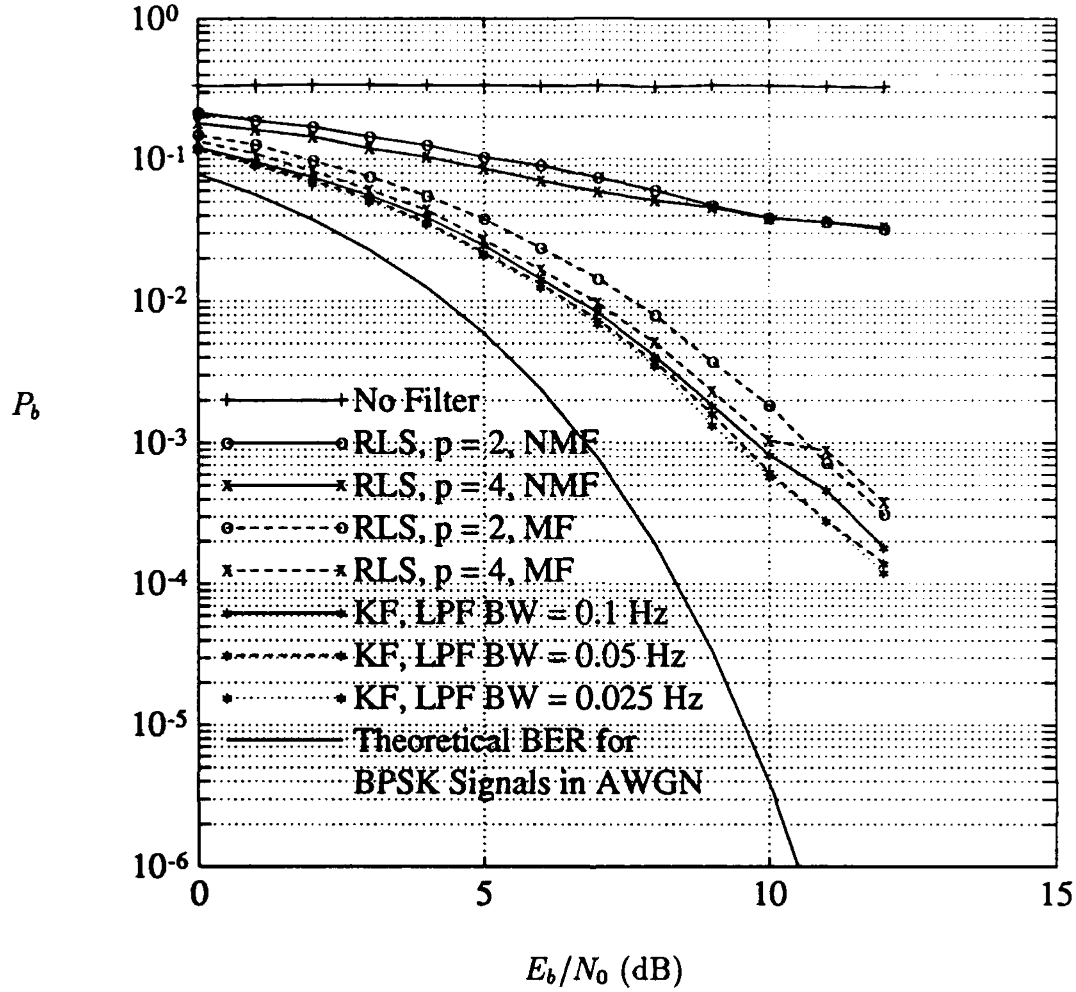

Figure 9: Comparison of the bit error rate performance between the RLS algorithm for $\lambda = 0.90$, and the Kalman filter algorithm for $d = 0.20$ rad./sec./volt and several values of low pass filter bandwidth (LPF BW) B_{LPF}. The acronymns NMF and MF respectively refer to "No Matched Filter" and "Matched Filter".

REFERENCES

[1] F. M. Hsu and A. A. Giordano, "Digital whitening techniques for improving spread spectrum communications performance in the presence of narrowband jamming and interference," *IEEE Transactions on Communications*, vol. 26, pp. 209–216, February 1978.

[2] J. W. Ketchum and J. G. Proakis, "Adaptive algorithms for estimating and suppressing narrowband interference in PN spread-spectrum systems," *IEEE Transactions on Communications*, vol. 30, pp. 913–924, May 1982.

[3] L. B. Milstein, "Interference rejection techniques in spread spectrum communications," *Proceedings of the IEEE*, vol. 76, pp. 657–671, June 1988.

[4] J. P. Burg, "Maximum entropy spectrum analysis," in *Modern Spectrum Analysis* (D. G. Childers, ed.), pp. 34–41, New York: IEEE Press, 1978.

[5] B. Widrow, J. M. McCool, M. G. Larimore, and C. R. Johnson, "Stationary and nonstationary learning characteristics of the LMS adaptive filter," *Proceedings of the IEEE*, vol. 64, pp. 1151–1161, August 1976.

[6] S. L. Marple, "A new autoregressive spectrum analysis algorithm," *IEEE Transactions on Acoustics, Speech, and Signal Processing*, vol. 28, pp. 441–454, August 1980.

[7] J. M. Cioffi and T. Kailath, "Fast, recursive-least-squares transversal filters for adaptive filtering," *IEEE Transactions on Acoustics, Speech, and Signal Processing*, vol. 32, pp. 304–337, April 1984.

[8] B. W. Kozminchuk, "Kalman filter-based architectures for interference excision," Technical Report 1118, Defence Research Establishment Ottawa, Ottawa, Ontario, Canada, K1A 0Z4, 1991.

[9] D. R. Polk and S. C. Gupta, "Quasi–optimum digital phase–locked loops," *IEEE Transactions on Communications*, vol. 21, pp. 75–82, January 1973.

[10] C. N. Kelly and S. C. Gupta, "The digital phase-locked loop as a near-optimum FM demodulator," *IEEE Transactions on Communications*, vol. 20, pp. 406–411, June 1972.

REFERENCES

[11] B. W. Kozminchuk, "Excision techniques in direct sequence spread spectrum communication systems," Technical Report 1047, Defence Research Establishment Ottawa, Ottawa, Ontario, Canada, K1A 0Z4, 1990.

[12] A. Blanchard, *Phase-Locked Loops.* New York: John Wiley and Sons, 1976.

[13] H. L. Van Trees, *Detection, Estimation, and Modulation-Part 2: Nonlinear Modulation Theory.* New York: John Wiley and Sons, 1971.

[14] R. E. Ziemer and W. H. Tranter, *Principles of Communications: Systems, Modulation, and Noise.* Boston: Houghton Mifflin Company, 1976.

DOCUMENT CONTROL DATA

(Security classification of title, body of abstract and indexing annotation must be entered when the overall document is classified)

1. ORIGINATOR (the name and address of the organization preparing the document. Organizations for whom the document was prepared, e.g. Establishment sponsoring a contractor's report, or tasking agency, are entered in section 8.)

DEFENCE RESEARCH ESTABLISHMENT OTTAWA
DEPARTMENT OF NATIONAL DEFENCE
SHIRLEY BAY, OTTAWA, ONTARIO K1A 0K2 CANADA

2. SECURITY CLASSIFICATION (overall security classification of the document, including special warning terms if applicable)

UNCLASSIFIED

3. TITLE (the complete document title as indicated on the title page. Its classification should be indicated by the appropriate abbreviation (S,C or U) in parentheses after the title.)

A COMPARISON OF RECURSIVE LEAST SQUARES AND KALMAN FILTERING EXCISORS FOR SWEPT TONE INTERFERENCE (U)

4. AUTHORS (Last name, first name, middle initial)

KOZMINCHUK, BRIAN W.

5. DATE OF PUBLICATION (month and year of publication of document)

OCTOBER 1992

6a. NO. OF PAGES (total containing information. Include Annexes, Appendices, etc.)

24

6b. NO. OF REFS (total cited in document)

15

7. DESCRIPTIVE NOTES (the category of the document, e.g. technical report, technical note or memorandum. If appropriate, enter the type of report, e.g. interim, progress, summary, annual or final. Give the inclusive dates when a specific reporting period is covered.)

DREO TECHNICAL NOTE

8. SPONSORING ACTIVITY (the name of the department project office or laboratory sponsoring the research and development. Include the address.)

DEFENCE RESEARCH ESTABLISHMENT OTTAWA
DEPARTMENT OF NATIONAL DEFENCE
SHIRLEY BAY, OTTAWA, ONTARIO K1A 0K2 CANADA

9a. PROJECT OR GRANT NO. (if appropriate, the applicable research and development project or grant number under which the document was written. Please specify whether project or grant)

041LK11

9b. CONTRACT NO. (if appropriate, the applicable number under which the document was written)

10a. ORIGINATOR'S DOCUMENT NUMBER (the official document number by which the document is identified by the originating activity. This number must be unique to this document.)

DREO TECHNICAL NOTE 92-14

10b. OTHER DOCUMENT NOS. (Any other numbers which may be assigned this document either by the originator or by the sponsor)

11. DOCUMENT AVAILABILITY (any limitations on further dissemination of the document, other than those imposed by security classification)

(XX) Unlimited distribution
( ) Distribution limited to defence departments and defence contractors; further distribution only as approved
( ) Distribution limited to defence departments and Canadian defence contractors; further distribution only as approved
( ) Distribution limited to government departments and agencies; further distribution only as approved
( ) Distribution limited to defence departments; further distribution only as approved
( ) Other (please specify):

12. DOCUMENT ANNOUNCEMENT (any limitation to the bibliographic announcement of this document. This will normally correspond to the Document Availabilty (11). However, where further distribution (beyond the audience specified in 11) is possible, a wider announcement audience may be selected.)

13. ABSTRACT (a brief and factual summary of the document. It may also appear elsewhere in the body of the document itself. It is highly desirable that the abstract of classified documents be unclassified. Each paragraph of the abstract shall begin with an indication of the security classification of the information in the paragraph (unless the document itself is unclassified) represented as (S), (C), or (U). It is not necessary to include here abstracts in both offical languages unless the text is bilingual).

(U) This technical note presents a Kalman filtering approach that is used for filtering narrowband interferers out of direct sequence spread spectrum signals. The approach is based on the digital phase-locked loop Kalman filter and is close to optimum in so far as demodulating an FM-type of interferer. Because the interference is assumed to be much stronger than either the signal or noise, the Kalman filter locks onto the interference and produces estimates of its phase and envelope. The algorithm is compared, through computer simulation, with the recursive least squares lattice algorithm for the case of a swept tone interferer. Examples of the phase- and envelope-tracking capabilities of the algorithm are presented, followed by bit error rate curves for the case of an interferer of bandwidth equal to 20% of the chip rate of the spread spectrum signal. The results show that with proper selection of the Kalman filter parameters, the Kalman filter excisor can outperform the recursive least squares algorithm by 2 dB. It is suggested that performance could perhaps be improved further by using a higher order Kalman filter to remove the residual phase-tracking error produced by the second order Kalman filter.

14. KEYWORDS, DESCRIPTORS or IDENTIFIERS (technically meaningful terms or short phrases that characterize a document and could be helpful in cataloguing the document. They should be selected so that no security classification is required. Identifiers, such as equipment model designation, trade name, military project code name, geographic location may also be included. If possible keywords should be selected from a published thesaurus. e.g. Thesaurus of Engineering and Scientific Terms (TEST) and that thesaurus-identified. If it is not possible to select indexing terms which are Unclassified, the classification of each should be indicated as with the title.)

LEAST SQUARES
RECURSIVE LEAST SQUARES
KALMAN FILTER
SPREAD SPECTRUM
INTERFERENCE SUPPRESSION
EXCISION